Edge Localized Modes as New Bifurcation in Tokamaks

Sanae-I. Itoh,[1] Kimitaka Itoh,[2] Atsushi Fukuyama,[3] and Masatoshi Yagi[1]
[1]*Research Institute for Applied Mechanics, Kyushu University 87, Kasuga 816, Japan*
[2]*National Institute for Fusion Science, Nagoya 464-01, Japan*
[3]*School of Engineering, Okayama University, Okayama 700, Japan*
(Received 18 September 1995)

A model of giant edge localized modes in tokamaks is developed. The theory of self-sustained turbulence of a current-diffusive ballooning mode is extended. A bifurcation from the H mode to a third state with magnetic braiding, the M mode, is found to occur if the pressure gradient reaches a critical value. Nonlinear excitation of magnetic perturbation takes place, followed by catastrophic increase of transport. With backtransition to the $H(L)$ mode, a new hysteresis is found in the gradient-flux relation. The process then repeats itself. Avalanche of transport catastrophe across the plasma radius is analyzed.

PACS numbers: 52.55.Fa, 52.25.Fi, 52.35.Kt

The H mode in tokamaks [1] is a bifurcation phenomenon in confined plasmas and is one of the typical examples for the structural transition in the system far from thermal equilibrium. This state is associated with the self-regulating dynamics, such as transition, transport barrier formation, and pulsating plasma losses. The latter dynamics, which are called edge localized modes (ELMs) [2], have attracted wide attention from the interest of nonlinear dynamics as well as of fusion research.

Various kinds of ELMs have been identified in experiments [2,3]. The small and frequent one, known as dithering ELMs, was explained in terms of a limit cycle due to the hysteresis characteristics in transport and electric field structure [4], based on the electric field bifurcation model of the H mode [5]. This picture has been confirmed by experiments [6]. At the same time, other kinds of ELMs, the repetitive occurrence of isolated giant bursts, have been widely observed. Due to a possibility of serious impact on the fusion device, this kind of ELM has been intensively studied in experiments. The condition for the occurrence of bursts was observed to be close to the stability boundary against the linear ideal ballooning mode [2,3,7]. However, it was noticeable that the magnetic fluctuations, which suddenly start to grow at the onset of the crash, change the growth rate abruptly without being preceded by a variation of the equilibrium plasma profile. This observation clarifies that the giant ELMs are essentially nonlinear and catastrophic events, not consequences of the growth of linear instabilities. Several theoretical efforts have been made as explanations [8,9], e.g., including the quasilinear dynamics of magnetohydrodynamic (MHD) mode [9]; however, the understanding of giant ELMs is far from satisfactory.

Recently, a new theoretical methodology for the plasma turbulence, i.e., the theory of self-sustained turbulence, has been developed to explain the L- and H-mode confinement [10,11]. In this framework, the possibility for the onset magnetic stochasticity and the catastrophe of transport was identified [12]. This is applied to the current diffusive ballooning mode (CDBM) in the presence of the radial electric field shear, which is relevant for the study of the H mode in tokamaks [5,13]. It is found that the self-sustained magnetic braiding, associated with the sudden enhancement of transport coefficient and fluctuation level, occurs if the pressure gradient exceeds a critical value. This new state ("M mode") persists until the pressure gradient becomes lower than another critical value. A new hysteresis in the flux-gradient relation is found, and the periodic dynamics consisting of a fast burst of fluctuations, a fast crash, followed by the slow buildup of pressure gradient is obtained. Contrary to previous ELM models [4,6,8,9], this new hysteresis exists even without including the flow shear dynamics. The critical pressure gradient is found to be close to experimental observations. The frequency of this cycle and the avalanche of transport catastrophe across the plasma radius are also analyzed. This mechanism not only explains giant ELMs in tokamaks but also serves as one typical example of the self-regulating dynamics in the nonlinear systems far from thermal equilibrium.

We study CDBM turbulence in high-aspect-ratio and circular tokamaks. To analyze self-sustained turbulence, the eigenvalue equation of the dressed-test mode was derived, in which nonlinear interactions are renormalized in a form of anomalous transport coefficients as [11]

$$\frac{d}{d\eta}\,\frac{F}{\hat{\gamma}+\hat{\lambda}n^4q^4F^2}\,\frac{d}{d\eta}\left(\hat{\gamma}+\hat{\chi}n^2q^2F+\omega_{E1}\frac{d}{d\eta}\right)\tilde{p}+\alpha[\kappa+\cos\eta+(s\eta-\alpha\sin\eta)\sin\eta]\tilde{p}-\left(\hat{\gamma}+\hat{\mu}n^2q^2F+\omega_{e1}\frac{d}{d\eta}\right)F\left(\hat{\gamma}+\hat{\chi}n^2q^2F+\omega_{E1}\frac{d}{d\eta}\right)\tilde{p}=0. \quad (1)$$

 0031-9007/96/76(6)/920(4)$06.00

The following notation is used: $\tilde{p}$ the perturbed pressure, γ the growth rate, n the toroidal mode number; χ, μ, and λ stand for thermal conductivity, viscosity, and current diffusivity, respectively, $F = 1 + (s\eta - \alpha \sin\eta)^2$, η the ballooning coordinate [14], $\alpha = -q^2 R\beta'$, $s = rq'/q$, q the safety factor, R the major radius, a the minor radius, $\omega_{E1} = E_r' \tau_{Ap}/B$, $\tau_{Ap} = qR/V_A$ (V_A being Alfvén velocity, and $\beta = 2\mu_0 p/B^2$. A caret indicates normalization $\hat{\gamma} = \gamma\tau_{Ap}$, $\hat{\mu} = \mu\tau_{Ap}a^{-2}$, $\hat{\chi} = \chi\tau_{Ap}a^{-2}$, and $\hat{\lambda} = (\delta/a)^2\hat{\mu}_e$, where δ is the collisionless skin depth. Although Eq. (1) was derived in the limit of $E \times B$ transport, the same equation is formally obtained in the limit of magnetic stochasticity [15] with different eigenvalues (χ, λ, μ).

Equation (1) determines the transport coefficient, the fluctuation level, and the scale length of fluctuations. The Prandtl numbers were found to be close to unity [10], and we set $\chi_e/\mu_e \sim \chi_i/\mu_i \sim 1$ here for simplicity. The transport coefficient was obtained as

$$\hat{\chi}_i = \frac{\alpha^{3/2}}{g(s,a)[1 + G(s,\alpha)\omega_{E1}^2]}\left(\frac{\delta}{a}\right)^2 \frac{\hat{\chi}_e}{\hat{\chi}_i}, \qquad (2)$$

where the coefficients g and G, which are of the order of 1 and 10, respectively, are given explicitly in [10,12] and are not repeated here.

In the H mode, (and the L mode as well, which is given by taking the limit of $\omega_{E1} \to 0$) the $\tilde{E} \times B$ transport dominates, and the relation $\hat{\chi}_e/\hat{\chi}_i \simeq 1$ holds. Introducing normalization as $\hat{\phi} = \tilde{\phi}/\varepsilon a v_A B_0$, $\hat{k}_{\theta,r} = ak_{\theta,r}$, $\hat{B}_r = \tilde{B}_r/\varepsilon B_0$, the static potential perturbation and the scale lengths were given as $\hat{\phi}_{H,L} = \hat{\chi}_{H,L}$, $\hat{k}_\theta = [g(1 + G\omega_{E1}^2)\alpha^{-1}]^{1/2}a/\delta$ and $\hat{k}_r = sg^{-1/2}(1 + G\omega_{E1}^2)^{1/4}\hat{k}_\theta$, respectively [11]. Ohm's law gives the relation between the static and magnetic perturbations as $\hat{B}_r = s(\hat{k}_\theta^2 a^2/\delta^2 \hat{k}_\perp^4 \hat{k}_r)\hat{\phi}/\hat{\chi}$. Substituting $\hat{k}_{r,\theta}$, we obtain the magnetic fluctuation amplitude in the H (L) mode as

$$\hat{B}_r^H = g^{-1}(1 + s^2 g^{-1}\sqrt{1 + G\omega_{E1}^2})^{-2}(1 + G\omega_{E1}^2)^{-7/4} \times \alpha^{3/2}\delta/a\,. \qquad (3)$$

Based on Eq. (3), the critical condition for the magnetic island overlapping is derived. The magnetic island size $\Delta_{\rm is}$ is estimated as $\Delta_{\rm is}/a = s^{-1}\hat{B}_r$ for the odd-ψ (even-ϕ) mode, where ψ is the parallel component of vector potential. The magnetic island width expands in proportion to $\alpha^{3/2}$. The separation distance of each rational surface d can be estimated by $\hat{d} \equiv d/a = (s\hat{k}_\theta)^{-1}$. It grows in proportion to $\alpha^{1/2}$. The Chirikov condition for island overlapping, $\hat{\Delta}_{\rm is} = \hat{d}/2$, is satisfied if the pressure gradient becomes high enough. Using Eq. (3), the threshold condition is given as

$$\alpha > \frac{\sqrt{g}}{2}(1 + G\omega_{E1}^2)^{5/4}(1 + s^2 g^{-1}\sqrt{1 + G\omega_{E1}^2})^2 \equiv \alpha_c^H\,. \qquad (4)$$

When α increases and reaches α_c^H, fluctuating islands overlap. The condition (4) shows that the critical value α_c^H is close to unity, and that it is increased by the magnetic shear or by the radial electric field shear.

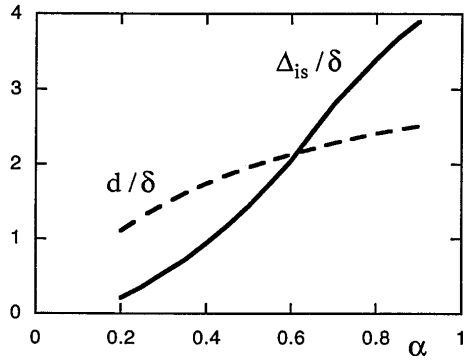

FIG. 1. Size of the magnetic island, $\Delta_{\rm is}$, and the separation distance of the mode rational surface d as a function of α. (Parameters $\delta/a = 10^{-2}$, $q = 3$, $\varepsilon = 1/8$, $s = 1.5$, and $\omega_{E1} = 0.12$.)

For comparison with experimental results, Eq. (1) is solved numerically. The solution for the least stable modes is obtained for given equilibrium parameters $(\alpha, s, \varepsilon, \ldots)$. The critical condition is calculated. In calculating $\hat{B}_r$, the evaluation $k_r^2 = n^2q^2\int_{-\infty}^{\infty}(s\eta - \alpha\sin\eta)^2\tilde{p}(\eta)^2 d\eta(\int_{-\infty}^{\infty}\tilde{p}(\eta)^2 d\eta)^{-1}$ is used with the solution of $\tilde{p}$. Figure 1 illustrates the island width and separation distance as a function of the pressure gradient. It confirms the α dependencies of $\Delta_{\rm is}$ and d, and demonstrates that the island overlapping condition is satisfied when α is of the order of unity. Figure 2 shows the critical conditions for the magnetic braiding in the s-α diagram. The thick solid line shows the case of weak radial electric field shear, and the thick dashed line indicates the stronger case. The critical boundary α_c^H increases approximately linearly in the high shear case. The M-mode transition disappears in low shear and high α region, where the second stability from the ideal MHD analysis has been predicted. For reference, the boundary for linear ideal ballooning instability is also shown, which turns out to be close to the boundary for nonlinear bifurcation.

When the magnetic perturbation is so large as to satisfy the Chirikov criterion, Eq. (4), the electron transport is more strongly enhanced than that of ions, $\chi_e \gg \chi_i$. Under these circumstances, Eq. (2) shows that the ion and electron transports are strongly enhanced from the H-mode (L-mode) transport. In the case for stochastic magnetic field, the turbulence renormalization gives the relation between the fluctuation level and transport coefficient as $\hat{\chi}_e^M = (v_{te}/v_{Ap})\varepsilon\hat{k}_r^{-1}M_s\hat{B}_r$, where v_{te} is the electron thermal velocity (see, e.g., [16]). When the electron decorrelation time due to transport $\tau_{\rm dec}^e$ is shorter than the transit time τ_t^e, i.e., $\tau_{\rm dec}^e/\tau_t^e < 1$, then $M_s \simeq \tau_{\rm dec}^e/\tau_t^e$ holds [17]. If $\tau_{\rm dec}^e/\tau_t^e > 1$, one has $M_s \simeq 1$, which was analyzed in [18]. Introducing the ratio M which is discussed later, the enhanced transport coefficient is expressed as

$$\hat{\chi}_e^M = \sqrt{m_i/m_e}M\hat{\chi}_i^M, \quad \hat{\chi}_i^{M_{H,L}} = \sqrt{m_i/m_e}M\hat{\chi}_{H,L}, \quad (5)$$

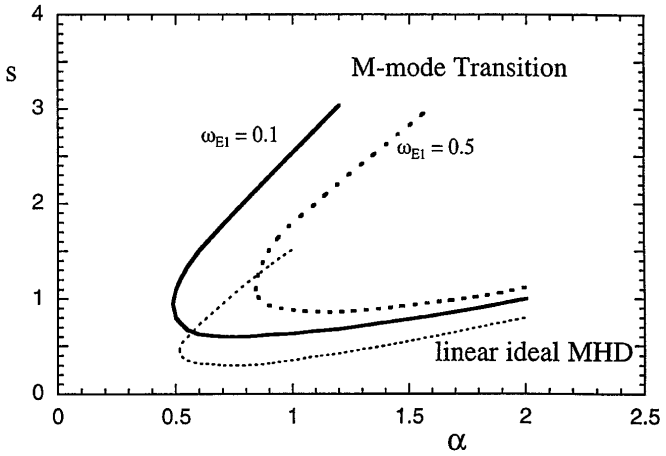

FIG. 2. Boundary of the H to M-mode transition in the s-α diagram. The thick solid line indicates the boundary for $\omega_{E1} = 0.1$ and the thick dashed line for $\omega_{E1} = 0.5$. The M-mode transition does not occur for the case of lower magnetic shear. The thin dotted line indicates, for reference, the linear ideal ballooning mode instability.

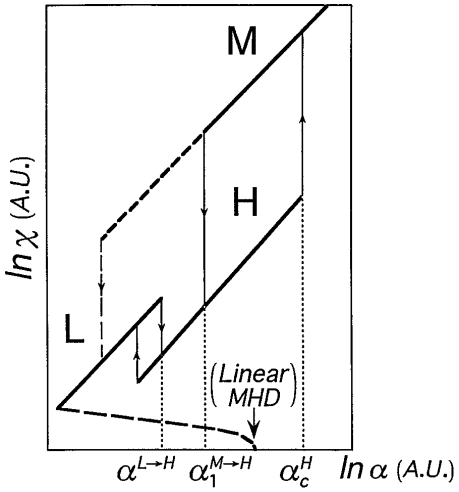

FIG. 3. Multifold solution of self-sustained turbulence. Thermal flux is shown as a function of the pressure gradient parameter α.

where $M \simeq \tau^i_{\rm dec}/\tau^i_t$ for $\tau^i_{\rm dec}/\tau^i_t < 1$ and $M_s \simeq 1$ for $\tau^i_{\rm dec}/\tau^i_t > 1$ [17]. This result is consistent with the one for the double streaming regime in [17].

The level and fluctuation scale lengths are calculated. In the M mode, the fluctuation scale length becomes longer, $(\hat{k}^M_\theta)^{-1} = (\hat{k}^H_\theta)^{-1}(M^2 m_i/m_e)^{1/4}$. For cases where the ratios $\hat{k}_\theta/\hat{k}_\perp$ and $\hat{k}_r/\hat{k}_\theta$ are unchanged from those in the H (L) mode, the magnetic perturbation is calculated as

$$\hat{B}^M_r = s g^{-1}(1 + G\omega^2_{E1})^{-1/4}(m_i/m_e)^{1/4} M^{3/2} M_s^{-1} q^{-1} \times \beta_i^{-1/2}\alpha(\delta/a), \quad (6)$$

where $\beta_i = v^2_{ti}/v^2_A$. The backtransition from the M to the H (L) mode is obtained by calculating the island width $\Delta^M_{\rm is}$ and the spacing of the rational surface d^M. Substituting Eq. (6) and $\hat{k}^M_{\theta,r}$, the condition $\Delta^M_{\rm is} > d^M/2$ can be rewritten as

$$\alpha \geq g s^{-2}(1 + G\omega^2_{E1})^{-1/2}(M_s/M)^2 q^2 \beta_i \equiv \alpha^M_1. \quad (7)$$

The region of the multifold branches is derived as $\alpha^M_1 \leq \alpha \leq \alpha^H_c$. The enhanced transport coefficient in the M state and the multifold branches in self-sustained turbulence provide a new hysteresis in the flux-gradient relation if $\alpha^M_1 < \alpha^H_c$. The schematic drawing of the various branches are shown in Fig. 3. The relation $\chi(\alpha; s)$ has the nature of cusp-type bifurcation, and the cusp point is determined by the relation $\alpha^M_1 = \alpha^H_c$. Hysteresis disappears if $\alpha^M_1 < \alpha^H_c$ is not satisfied.

A cycle, the sequence of which consists of (1) the buildup of pressure gradient in H mode, (2) the H-to-M transition at $\alpha = \alpha^H_c$, (3) the crash of plasma profile by the M-mode transport, and (4) the backtransition to the H at $\alpha = \alpha^M_1$, is attributed to a giant ELM. At some location near the edge $r = r_{\rm Ch}$, the Chirikov condition for the magnetic island overlapping, $\alpha = \alpha^H_c$, could be first satisfied. A catastrophic transition sets in, and the rapid electron loss occurs and the fast ion loss is caused as well: The electron and ion energy, as well as the density, collapse. The time scale for the turbulence growth $\hat{\tau}_{\rm gr}$ is given by the inverse of the nonlinear growth rate [10] as $\hat{\tau}_{\rm gr} \sim s^{1/3} g^{1/6}(1 + s^2 g^{-1})^{-1/3}\alpha^{-1/2}$, being the order of the poloidal Alfvén time. Pressure is increased outside ($r > r_{\rm Ch}$) and is reduced inside ($r < r_{\rm Ch}$). Thus the pivot point of the pressure perturbation is close to the radius $r = r_{\rm Ch}$.

The chained M-mode transitions propagate from $r = r_{\rm Ch}$. The typical time scale of the avalanche is order estimated from a simple model of dominos. The time for profile change at $r = r_{\rm Ch}$ is given roughly by $\tau^M_c = (\ell^M_r)^2/\chi^M_e$, and the steepening of pressure gradient is induced at $r \simeq r_{\rm Ch} \pm \ell^M_r$, leading to the onset of critical condition at these locations. [The scale length ℓ^M_r is given as $(k^M_r)^{-1}$.] The transport catastrophe propagates at the speed of the order of $V_{\rm ava} \simeq \ell^M_r/\tau^M_c$. If the avalanche occurs in the region $r_p < r < r_{\rm Ch}$, the propagation time is given by $\tau_{\rm ava} = (r_{\rm Ch} - r_p)\tau^M_c/\ell^M_r$. It is much faster than the diffusion time of the L phase, $\tau^L_{\rm diff} = (r_{\rm Ch} - r_p)^2/\chi^L_e$. The location r_p could be the place where the hysteresis disappears, i.e., $\alpha^M_1(r_p) = \alpha^H_c(r_p)$.

Finally, the period of ELM bursts is derived. The periodic dynamics occurs if the power across the plasma surface, $P_{\rm out}$ exceeds the threshold value, $P^{\text{G-ELM}}_{\rm th} = (2\pi^2 a R B^2/\mu_0 q^2 R)\chi_H(\alpha^H_c)\alpha^H_c$. The frequency of ELMs $\nu_{\rm ELM}$ is given as $\nu_{\rm ELM} \simeq (\tau_H + \tau_{\rm gr} + \tau^M_c)$, where τ_H is the time during which the value of α increases from α_1 to α^H_c. Since $\tau_{\rm gr}$ and $\tau_{\rm ava}$ are much shorter than τ_H, the ELM period is approximated as $\nu_{\rm ELM} \simeq \tau^{-1}_H$. An analytic estimate of $\nu_{\rm ELM}$ is given by balancing the input and loss energies as $P_{\rm out}/\nu_{\rm ELM} \simeq (4\pi^2 a\Delta^2 B^2/2\mu_0 q^2)(\alpha^H_c - \alpha^M_1)$ for $P_{\rm out} \gg P^{\text{G-ELM}}_{\rm th}$ (where Δ is the typical radial width of the ELM, $\Delta \simeq a - r_p$), showing that $\nu_{\rm ELM} \propto P_{\rm out}$ if $(4\pi^2 a\Delta^2 B^2/2\mu_0 q^2)(\alpha^H_c - \alpha^M_1)$ is a weak function of $P_{\rm out}$. The dependence of $\nu_{\rm ELM}$ on other parameters could be derived from this relation.

In summary, we presented a theoretical model of a giant ELM as a bursting phenomenon caused by the M-mode transition inside the plasma edge. The cycle of burst and recovery is attributed to the type-I ELM. The M-mode is a transient phase of giant ELMs during which the field lines become stochastic because of violation of Chirikov criterion. This model explains several features of the giant ELM: the sudden crash, rapid radial propagation, the power dependence of the period, the critical pressure gradient $\alpha = \alpha_c^H$ for the onset, and the disappearance in the second stability region against the ballooning mode. The criterion could be close to the ideal beta limit without taking the E_r' effects into account. The criterion in high-shear limit in Fig. 2, $\alpha_c^H \sim s/2$, is close to the experimental observations [7]. The gradient-flux relation in Fig. 3 gives a general picture in a phenomenology of the H mode. Near the threshold power for the L-H transition, $P_{\rm out} \sim P_{\rm th}^{L/H}$, the limit cycle (dithering ELMs) takes place [5]. In the region $P_{\rm th}^{L/H} \ll P_{\rm out} \leq P_{\rm th}^{\text{G-ELM}}$, the stationary solution is realized, which corresponds to the ELM-free H mode. In the case of the larger power flux $P_{\rm out} \geq P_{\rm th}^{\text{G-ELM}}$, the giant ELMs are predicted to occur.

In the presence of the inhomogeneous radial electric field, the 1D eigenvalue equation in the ballooning coordinate [Eq. (1)] would be allowed in a small ω_{E1} limit, but must be treated in 2D form in general [19]. This may change the critical value of α quantitatively. The other issue is the self-consistent determination of M_s and M. In the case of $\tau_t^j \leq \tau_{\rm dec}^j$ ($j = e$ and i), the transit time is given as $\tau_t^e = L_{\rm ac}/v_{\rm the}$, where the autocorrelation length of the magnetic perturbation $L_{\rm ac}$ has the relation $\tilde{B}_r/B \cong 1/L_{\rm ac}k_r$ [17]. By estimating the decorrelation time as $(\tau_{\rm dec}^e)^{-1} \sim \chi_e^M (k_\theta^M)^2$, one can estimate M and M_s [20] as $M_s \sim 1$ and $M \sim (\beta_i \alpha)^{1/2}$. Substituting this M into Eq. (5), we confirm that the form of χ_i^M is consistent to the result by the scale invariance on the ballooning mode with magnetic braiding [21]. (Note that the constraint such as [22] does not apply here, because the turbulent decorrelation rate is larger than the mode frequency.) For the typical value of the experiments, $\alpha \sim 1$ and $\beta_i \sim (1\text{–}0.1)\%$, we have $M \sim 1/10\text{–}1/20$. The electron and ion transport coefficients in the M state are enhanced by the factor of approximately 20 and 5 times, respectively, from those in L mode. These estimates for M and M_s allow the hysteresis to exist, $\alpha_1 < \alpha_c$, if the M-mode transition is possible in Fig. 2, i.e., s is greater than unity or so.

Variations in ω_{E1} and s would allow new paths of development and more complicated oscillation phenomena. The magnitude of the ELM event depends on the location of the end of avalanche r_p, the determination for which requires global solution for profiles. A detailed study of dynamics near the marginal condition of transport change was given in [23]; such an investigation would be essential for the case of $P_{\rm out} \sim P_{\rm th}^{\text{G-ELM}}$ and must be extended to this model with hysteresis. This theory could be altered if the tearing modes are unstable, suggesting the necessity of careful study on the edge current profile. The study on the ion mass effects on the H-mode performance was started [24], and the impact on ELMs will be discussed in the future. For the explanation of the type-III ELMs, another theory would be necessary. This is left for future analysis.

The authors acknowledge discussion on experimental data with Professor F. Wagner, Dr. Y. Miura, JFT-2M Group, Dr. H. Zohm, ASDEX-U Group, Dr. K. H. Burrell, DIII-D Group, Dr. T. Takizuka, and JT-60U Team. This work is partly supported by the Grant-in-Aid for Scientific Research of the Ministry of Education in Japan.

[1] ASDEX Team, Nucl. Fusion **29**, 1959 (1989).
[2] M. Keilhacker *et al.,* Plasma Phys. Controlled Fusion **26**, 49 (1984).
[3] E. J. Doyle *et al.,* Phys. Fluids B **3**, 2300 (1991).
[4] S.-I. Itoh *et al.,* Phys. Rev. Lett. **67**, 2485 (1991).
[5] S.-I. Itoh and K. Itoh, Phys. Rev. Lett. **60**, 2276 (1988).
[6] H. Zohm, Phys. Rev. Lett. **72**, 222 (1994).
[7] P. Gohil *et al.,* Phys. Rev. Lett. **61**, 1603 (1988); T. Ozeki *et al.,* Nucl. Fusion **30**, 1425 (1990).
[8] S.-I. Itoh *et al.,* Nucl. Fusion **33**, 1445 (1993).
[9] P. H. Diamond *et al., Proceedings of the International Conference on Plasma Physics and Controlled Nuclear Fusion Research* (IAEA, Seville, 1994), Paper D-2-II-6; V. B. Lebedev *et al.,* Phys. Plasmas **2**, 3345 (1995).
[10] K. Itoh *et al.,* Plasma Phys. Controlled Fusion **36**, 279 (1994).
[11] S.-I. Itoh *et al.,* Phys. Rev. Lett. **72**, 1200 (1994).
[12] K. Itoh, A. Fukuyama, S.-I. Itoh, and M. Yagi, Plasma Phys. Controlled Fusion **37**, 707 (1995).
[13] S.-I. Itoh *et al., Plasma Physics and Controlled Nuclear Fusion Research 1988* (IAEA, Vienna, 1989), Vol. 2, p. 23; H. Bigrali *et al.,* Phys. Fluids B **2**, 1 (1990).
[14] J. W. Connor, R. J. Hastie, and J. B. Taylor, Proc. R. Soc. London A **365**, 1 (1978).
[15] M. Yagi *et al.* (to be published).
[16] C. W. Horton, in *Basic Plasma Physics II,* edited by A. A. Galeev and R. N. Sudan (North-Holland, Amsterdam, 1984), Sect. 6.4.
[17] See, e.g., J. Krommes *et al.,* J. Plasma Phys. **30**, 11 (1983).
[18] A. B. Rechester and M. N. Rosenbluth, Phys. Rev. Lett. **40**, 38 (1978).
[19] F. Wealbroeck *et al.,* Phys. Fluids B **3**, 601 (1991).
[20] S.-I. Itoh *et al.,* "A model of Giant ELM" (to be published).
[21] J. W. Connor, Plasma Phys. Controlled Fusion **35**, 757 (1993).
[22] P. W. Terry *et al.,* Phys. Rev. Lett. **57**, 1899 (1986).
[23] P. H. Diamond *et al.,* Phys. Plasmas **2**, 3640 (1995).
[24] K. Itoh and S.-I. Itoh, Plasma Phys. Controlled Fusion **37**, 491 (1995).